Transactions on the Built Environment vol 53, © 2001 WIT Press, www.witpress.com, ISSN 1743-3509

# Fish and ships: can fish inspired propulsion outperform traditional propulsion based systems?

A. Manuello Bertetto, B. Picasso and M. Ruggiu
*Dipartimento di Ingegneria Meccanica,*
*Università di Cagliari, Italy.*

## Abstract

Fish propulsion mechanism is becoming a major research topic. Effort is aimed at understanding the reasons for the high swimming performances of marine creatures and investigating the possibility of applying fish-like propulsion to surface and underwater vehicles.
In this paper, two mathematical models were developed and applied to predict thrust in oscillating tail propulsion. The former was based on the classical treatment of M.J. Lighthill, the latter on the calculation of the instantaneous airfoil kinematics and dynamics by means of a numerical procedure. A fish robot prototype and a thrust measuring equipment were developed in order to assess the accuracy and reliability of the analytical models used. The comparison of the analytical and measured thrust values showed that the average thrust values calculated both according to the Lighthill theory and the numerical model well approximate the experimental values. The numerical model falls short in giving a full quantitative evaluation of the thrust, while it gives a convincing qualitative picture of the thrust production cycle. The simplifications and assumptions made are discussed in order to justify some weaknesses of the models used.

## 1 Introduction

Natural selection ensured that the propulsion systems evolved in fish are highly efficient. Their remarkable swimming abilities could inspire innovative and efficient designs to improve the ways man-made systems operate in the aquatic environment. The swimming strategy of fishes can provide inspiration for a design that could possibly outperform the current naval propulsion systems: for nimble underwater and surface vehicles, the existing propulsion devices could be unsatisfactory when it comes to demanding particular applications. In addition,

the advantages of noiseless propulsion could be of significance, particularly for military applications.
Some mobile marine robotic devices are currently being developed to assess the potential and study the propulsive kinematic patterns utilised by fish and other aquatic animals [1], [2], [3], [4]. Generally, fish that use the same propulsion method display similar morphology. Webb identified three basic architectures of fish morphology, derived from the specialisations for accelerating, cruising, and maneuvering [5]. Lighthill in [6], [7], [8], [9] proposes a model for fish propulsion mechanics which takes into account some of the most important features of the body geometry of fast swimming fish. Lighthill's model is based on the fact that, with the undulating transverse movement of its body, the fish pushes a surrounding mass of water. For each elementary slice of the fish body, this mass can be considered to be equivalent with that of a water cylinder whose diameter is equal to the height of the section including ventral and dorsal fins. While the fish is moving forward, the oscillatory movement of the fin produces a double vortex sheet analogous to the classical Karman wake. A propulsion force can also be obtained for a more general law of movement, consisting of a translation of the fin centre of mass and of a rotation around it. This general law of movement has been studied by Von Karman and Garrick [10].
The wake left behind the fin is an array of discrete vortices of alternating sign, generated as the caudal fin moves, producing a backward water jet. The structure of the wake is of a thrust-type, it is reversed compared to the drag-producing Karman vortex sheet, typically observed in the wake of objects moving in a fluid [11].
The attractive features of the oscillating fin propulsion have fostered many efforts to develop propulsion systems using fish-like motion patterns. Interesting examples are reported in the [12-16] web sites, where different devices are presented. Commercially the interest in fish-like propulsion is testified by the financial engagement of important Shipbuilding Companies like the four-year project at Mitsubishi Heavy Industries.

## 2 Mechanics of Motion and Analytical Model

According to the Von Karman approach the lift due to the non stationary motion of a thin airfoil is the sum of three terms:

1. Quasi steady lift.
2. The inertial component.
3. The contribution of the wake.

The basic assumptions were of the two dimensional flow field, small transverse oscillations, and applicability of thin airfoil aerodynamics. More than 35 years later the milestone paper by M.J.Lighthill [8] presented an extensive analysis of fish propulsion mechanics. Lighthill classifies fish into two large families from the propulsion point of view: anguilliform (eel shaped) and carangiform. The basic distinction between them is that eel shaped fish propel using a backpropagating transverse wave involving the whole body, whereas carangiform fish propel simply by oscillating the tail fin. The results obtained by Lighthill are given as curves which represent the variation of the thrust coefficient $C_T$, defined as the thrust per unit of projected fin area and per unit of fluid kinetic energy versus the reduced frequency $\Omega$ and the feathering parameter $\theta$:

$$C_t = \frac{T}{0.5 \cdot S \cdot \rho \cdot w^2}; \quad \Omega = \frac{\omega \cdot c}{U}; \quad \vartheta = \frac{U \cdot \alpha}{\omega \cdot h} \tag{1}$$

where T is the thrust, S the projected fin area, w the relative water velocity, $\omega$ is the radian oscillation frequency of the tail beat, c is the chord length of the hydrofoil and U is the fish forward speed. The feathering parameter $\theta$ is the ratio between the amplitude of the tail angular oscillation $\alpha$ and the incidence angle $(\omega \cdot h)/U$, h being the transverse displacement of the hydrofoil midpoint.

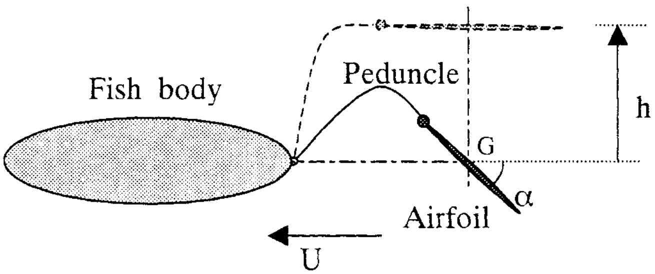


Figure 1: Fish tail geometry and parameters

In using Lighthill's results, in the present work it was assumed that the lunate tail was made of a peduncle connecting the airfoil section to the fish body. As a consequence of that the generally negative contribution of the peduncle to the total thrust was neglected . The comparison of the thrust mean values obtained using Lighthill's model with the experimental results, will be given in section 5.

## 3 The Robot

The robot fish [4] consists of four parts: a cylindrical aluminum body with a 160 mm diameter, a front fiberglass nose, a rear conical part containing the motor and transmission, and a tail. The motor is powered by two Pb-batteries (12V, 1Ah) which are placed in the central section. The motion law is controlled by a microcontroller. The mechanical transmission consists of a couple of bevel gears and a toothed belt. The tail is made of polycarbonate and its shape was replicated from a real tuna tail fin. The frequency of the tail motion was varied up to a 3 Hz maximum.

Transactions on the Built Environment vol 53, © 2001 WIT Press, www.witpress.com, ISSN 1743-3509



# 4 Numerical Model

The robot kinematics and dynamics were simulated by using a commercial code [18] based on the numerical integration of the motion equations. The tail was modeled by a two degrees of freedom planar body made by a peduncle and a hydrofoil, neglecting three dimensional effects. The robot casing was modeled by a planar body having its mass whereas the dynamometer was substituted by a spring-dashpot unit whose stiffness and the damping coefficients were deduced by some vibration tests. Therefore, the complete model consists of three degrees of freedom. Although the real fish tail deforms in a complex fashion such a model was considered to be adequate to describe the basic mechanisms of lift and drag generation. In figure 2 the model free-body diagram is shown:

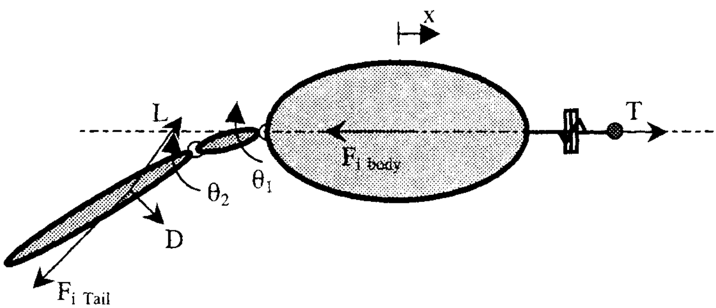


Figure 2: Free body diagram of the system

The lift, drag and inertial force acting on the tail can be seen. The application point of the lift and drag was assumed to be at 1/4 of the chord length. Their absolute values were numerically calculated using $C_D$ and $C_L$ data measured on the tail fin immersed in a stationary flow at different incidence angles (section 5). The inertial force involved in the calculations was based on a virtual mass corresponding to the water volume of a cone surrounding the tail fin. Since the motion kinematics was calculated stepwise, the above forces are fully individuated. The thrust exerted by the tail is calculated as the tension in the spring-dashpot unit. In so doing only the component of the inertial force due to the tangential tail acceleration could be considered.

# 5 Experimental

Numerous tests were conducted in order to measure the thrust exerted by the robot propulsion system with different motion parameters. Moreover specific tests were carried out for measuring the lift and drag of the tail.
In figure 3 the test apparatus developed for thrust measurements is shown:

Transactions on the Built Environment vol 53, © 2001 WIT Press, www.witpress.com, ISSN 1743-3509



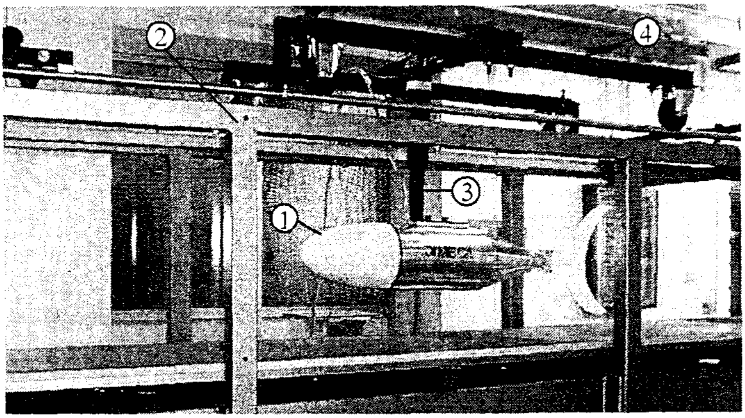


Figure 3 : Test apparatus for thrust measurement

The above picture shows the robot (1) immersed in the water canal (2). The robot body is fixed to a dynamometer beam (3) which is constrained to a mobile cart (4) fixed to on top of the canal structure. The following measurements were carried out: velocity of the water using an anemometer located upstream of the fish robot, tail position using a transducer mounted onto the motor shaft, bending strain using the strain-gages placed on the top of the dynamometer. The signals were acquired in real time and sent to a computer. The robot thrust was obtained by multiplying the strain by the calibration factor. In order to detect this factor an accurate calibration procedure of the dynamometer was worked out by using a calibrated load cell.

## 5.1. Lift and Drag Measurement

In order to accurately model the tail dynamics, the lift and drag coefficients $C_L$, $C_D$ were experimentally evaluated. The tail was mounted at different incidence angles, from 0° through 35°, with respect to the dynamometer axis. The dynamometer sensitivity direction was aligned with the canal axis when measuring the drag force, whereas it was rotated by 90° for obtaining the lift. The measurements were repeated for three different water velocities: 0.18 m/s, 0.24 m/s, 0.44 m/s. Finally the $C_L$ coefficient was obtained by dividing the lift by the constant $0.5 \cdot S \cdot \rho \cdot w^2$ where S is the fin cross section, ρ is the water density and w is the velocity of the water with respect to the fin, in this case, coinciding with the absolute water velocity U. A similar procedure was performed for the $C_D$ coefficient. In figure 4 below the experimental $C_L$, $C_D$ curves vs. the incidence angle are shown:

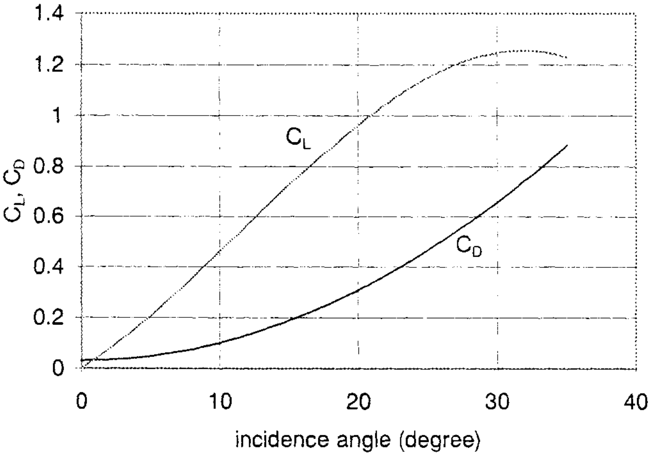


Figure 4: Lift and Drag Coefficients vs. incidence angle

It can be noted that $C_L$ reaches its maximum of about 1.2 at a 30° incidence angle whereas $C_D$ presents its minimum of 0.03 at 0°.

### 5.2. Thrust Measurements

Numerous tests were performed in order to measure the thrust exerted by the robot with different frequencies and amplitudes of the tail motion. The experiments were carried out with different water velocities as well. As an example in figure 5 below the thrust vs. time curve at f=1.25 Hz and semi-amplitude $\alpha$=12.5° is shown. It is worth emphasising that in a complete tail cycle (forward-backward) the thrust curve reaches its maximum twice when the tail does pass over the mid-side position. Moreover it can be observed that the thrust assumes negative values during the tail cycle as well.

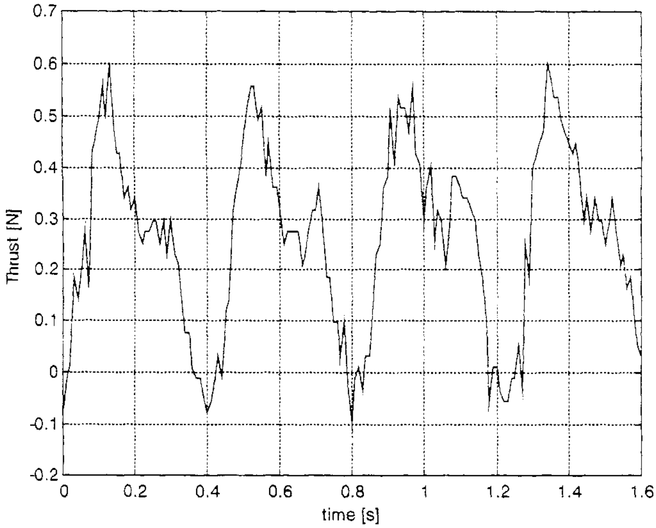


Figure 5: Thrust vs. time curve with f=1.25 Hz, $\alpha$=12.5°

Because of the proximity of the system (dynamometer-robot) resonant frequency to the tail motion frequency, some experimental data were post-processed and filtered in order to eliminate the system frequency component into the thrust signal. In table 1 below, for a 0.2 m/s water velocity of and under different motion conditions, the mean value of the thrust is given, together with the corresponding predicted values:

Table 1. Experimental and calculated average thrust values

| f (Hz) | 0.8 | 0.8 | 0.8 | 0.8 | 1.25 |
|---|---|---|---|---|---|
| $\alpha$ (deg) | 12.5 | 20 | 30 | 40 | 12.5 |
| $\theta$ | 0.268 | 0.270 | 0.278 | 0.288 | 0.171 |
| h (m) | 0.0324 | 0.0513 | 0.075 | 0.0964 | 0.0324 |
| Lighthill | 0.13 | 0.31 | 0.681 | 1.12 | 0.32 |
| Num. Model | 0.178 | 0.256 | 1.9 | 2.6 | 0.30 |
| Test results | 0.175 | 0.25 | 0.39 | 0.19 | 0.26 |

It is worth emphasising that both the analytical and numerical methods are in good agreement with the experimental data for small tail motion amplitudes. A great discrepancy was found when $\alpha$ is higher than 20°.

Referring to the motion condition of f=0.8 Hz and $\alpha$=20°, in figure 6 a comparison between the obtained numerically thrust and that measured during a tail cycle is given.

Transactions on the Built Environment vol 53, © 2001 WIT Press, www.witpress.com, ISSN 1743-3509



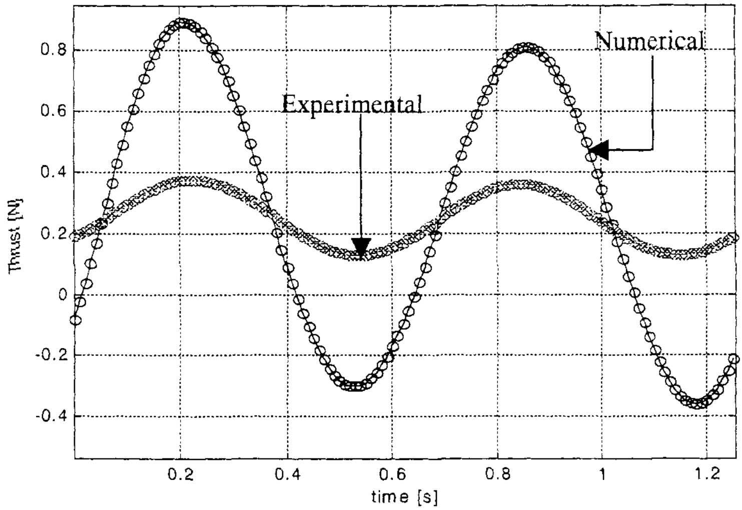


Figure 6: Numerical and experimental Thrust vs. time curves

It can be observed that the model misses the magnitudes of the peaks in the thrust curve. For the motion condition described above, the numerical thrust maxima were about twice the experimental values. That can be explained by means of the enormous simplifications introduced into the numerical model. In particular it must be pointed out that the lift formula does not consider the occurrence of stall when the incidence angle becomes grater than 35°.

Despite these results, the thrust trend with time is fully captured by the model. Moreover the thrust mean value obtained numerically approximate the experimental value. For example, for the motion conditions of figure 6, the error calculated between the numerical and experimental mean values is under 5%.

## 6 Conclusions

A strong research endeavour is needed to reach a full understanding of the real potential of fish inspired propulsion for marine applications. In this paper it has been shown that relatively simple models can be used to predict the average thrust values produced by an oscillating fin. Moreover the implementation of a fully instrumented test rig permitted to get a fruitful insight into many aspects of the propulsion mechanics. The applicability of the models used seems to be limited to small angular oscillations, say less than 30°of half angular amplitude. Further investigations are planned to develop improved models with extended applicability.

# Bibliography


[1] D. Barrett, M. Grosenbaugh, and M. Triantafyllou, "The optimal control of a fexible hull robotic undersea vehicle propelled by an oscillating foil," in *Proc. 1996 IEEE AUV Symp.*, pp. 1–9.

[2] N. Kato and M. Furushima, "Pectoral fin model for manuever of underwater vehicles," in *Proc. 1996 IEEE AUV Symp.*, pp. 49–56.

[3] I. Yamamoto, Y. Terada, T. Nagamatu, and Y. Imaizumi, "Propulsion system with exible/rigid oscillating fin," *IEEE J. Oceanic Eng.*, vol. 20, pp. 23–30, 1995.

[4] B. Picasso, A. Manuello Bertetto, M. Ruggiu, "Development of a robotic Fish for Surface and Underwater Inspection: an Experimental Study on the Mechanics of Oscillating Tail Propulsion", in *Proc. 9th International Workshop on Robotics in Alpe-Adria-Danube Region RAAD 2000*, pp. 227-232.

[5] P.W. Webb, "Form and function in fish swimming," *Sci. Amer.*, vol. 251, pp. 58–68, 1984.

[6] M.J. Lighthill, "Note on the swimming of slender fish", *Journal of Fluid Mechanics*, vol. 9, 1960.

[7] M.J. Lighthill "Hydromechanics of aquatic animal propulsion", *Journal of Fluid Mechanics*, vol. 44, 1969.

[8] M.J. Lighthill "Aquatic Animal Propulsion of High Hydromechanical Efficiency", *Journal of Fluid Mechanics*, vol. 44, 1970.

[9] M.J. Lighthill, "Large amplitude, elongated body theory of fish locomotion", in *Proc. R. Soc. Lond. Ser. B. Biol.Sci., pp.* 125-138, 1971.

[10] Garrick I.E., "Propulsion of A Flapping And Oscillating Airfoil", *NACA Technical Report 567, 1936.*

[11] G. S. Triantafyllou, M. S. Triantafyllou, and M. A. Grosenbauch, "Optimal thrust development in oscillating foils with application to fish propulsion," *J. Fluids Struct.*, vol. 7, pp. 205–224, 1993.

[12] http://www.cee.hw.ac.uk/~sfakios/html/describe.htm
web page of Heriot-Watt University (Edinburgh – Scotland)

[13] http://www.erc.caltech.edu/Research/Reports/mason1full.html
web page of Caltech - Center for Neuromorphic Systems Engineering

[14] http://dimeca.unica.it/labrob.html
DIMECA University of Cagliari Italy robotic lab web page

[15] http://web.mit.edu/towtank/www/tuna/brad/tuna.html
MIT web page Massachusetts USA

[16] http://robby.caltech.edu/~kristi/
Caltech web page California USA

[17] http://draper.com/tuna_web/vcuuv.htm
Draper Laboratories web page

[18] Working Model 2D User's Manual, Knowledge Revolution Inc.